# An Adaptive High-Precision Tracking Controller for the Coupled Switched Reluctance Two-Finger Gripper

Y. Zou[1,2], Norbert C. Cheung[2], and J. F. Pan[1]

[1]Shenzhen Key Laboratory of Electromagnetic Control, Shenzhen University, Shenzhen 518060, China
[2]Department of Electrical Engineering, The Hong Kong Polytechnic University, Hong Kong

**An adaptive high-precision position control algorithm with online system identification is implemented onto the switched reluctance, two-finger gripper with coupled magnetic paths. Theoretical investigation proves that the magnetic paths from the two fingers are highly coupled. Without the introduction of any decoupling scheme, the position control performance under the proportional integral differential controller and the adaptive controller is inspected and the control results are compared. Experimental results verify that, without introducing any decoupling mechanism, the adaptive controller is capable of independent control of each finger with a high-precision and uniform position control performance.**

*Index Terms*—**Adaptive control, gripper, system identification.**

## I. Introduction

FINGER grippers play an important role in the modern industry, and they have become indispensible for mankind to maneuver in the automation fields, such as hazardous material handling, postdisaster rescues, and so on [1], [2]. With the fast development of semiconductor industry, the demand for high-precision, reliable, and robust finger grippers are growing [3]. Therefore, low-cost, mechanically stable finger grippers and their motion control systems should be developed with high reliability and good performance for such applications.

At present, various types of finger grippers have been developed and investigated. These include direct current (dc), dc brushless, piezoelectric, and voice coils grippers. In a dc gripper, velocity and torque can be linearly regulated by the terminal voltage and the armature current [3]. This makes the dc gripper a favorable solution for the motion control system. However, due to the presence of commutation brushes, dc grippers require frequent maintenance, and the electrical noise from the brushes emits continuous interference to the environment [4]. An alternative is to use a dc brushless gripper with electronic commutation method instead of mechanical brushes. Without any electrical contact between the stator and the rotor, the generated electrical noise can be decreased significantly [5]. However, with the involvement of permanent magnets (PMs), the dc brushless can only operate within a limited temperature range, and the PMs can be permanently demagnetized in some hostile operation environment [6]. Though a piezoelectric gripper has a compact size and offers high precision, it should be linked up with mechanical displacement transfer elements to provide gripping motions [7]. The output force is low and the grippers often suffer from small opening areas; therefore, they can merely be employed in miniature mechatronic systems [7].

The switched reluctance (SR) machines have drawn researchers' attention, owing to their simple and robust mechanical structure. The proposed SR two-finger has the features of maintenance-free, and it is capable of operation in a wide temperate range [8]. However, the gripper exhibits inherent uncertainties and external disturbances, such as manufacture and assembly imperfections, winding resistance change, frictional force variations, load change, and so on. There is a severe coupling between the shared magnetic paths. In addition, the spring pulling effect acts as an undesirable variable load to the control system. Therefore, the traditional proportional integral differential (PID) position regulator is not capable of decoupling and precise trajectory tracking for the two grippers working at the same time. To achieve a high-precision position control performance, a dynamic model that reflects system uncertainties and external disturbances is required for a uniform operation of the gripper. With online system identification, the parameters of the plant model can be obtained in real time. The adaptive position controller based on the pole placement design is applied for real time compensation of system uncertainties and external disturbances.

TABLE I
Major Specifications

| Parameter | Value |
|---|---|
| Number of turns | 200 |
| Winding resistance | 3 Ω |
| Air gap length | 0.5 mm |
| Stroke angle | 45° |
| Spring coefficient | 70 N/m |
| Encoder resolution | 0.009° |

## II. Structure and Modeling

The SR gripper mainly consists of a pair of windings, aluminum housing, fixture and supporters, and laminated silicon-steel plates for the stator and rotor to reduce eddy current effects. The left and right grippers with rotors have the double rotating axes, with each axis mounted on an individual shaft. Both fingers have the same dimensions and ratings. Detailed information of the SR gripper can be found in Table I. A pair of incremental encoders is mechanically connected to each rotating shaft, as shown in Fig. 1(a). When the left finger gripper is excited, flux lines will be established along the stator, the left rotor, and the air gap.

Manuscript received March 19, 2015; revised May 10, 2015; accepted May 19, 2015. Date of publication May 21, 2015; date of current version October 22, 2015. Corresponding author: J. F. Pan (e-mail: pan_jian_fei@163.com).

Color versions of one or more of the figures in this paper are available online at http://ieeexplore.ieee.org.

Digital Object Identifier 10.1109/TMAG.2015.2436399

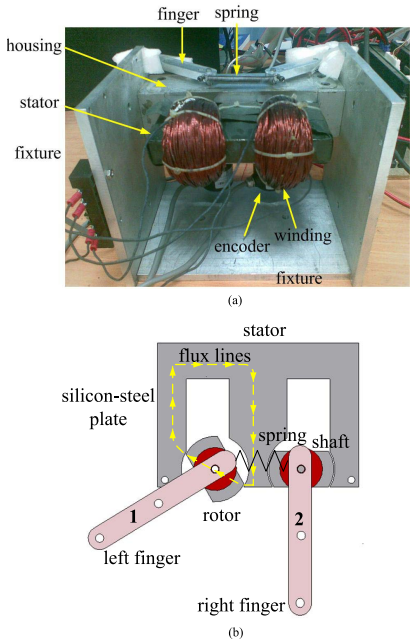


Fig. 1. Gripper prototype. (a) A pair of incremental encoders is mechanically connected to each rotating shaft and (b) The exited rotor with the finger will turn anti-clockwise until it is fully aligned with the stator.

The exited rotor with the finger will turn anticlockwise until it is fully aligned with the stator, as shown for the right finger position in Fig. 1(b). For backward movement, each gripper is attached to a torsional spring.

Since each finger has the same dimensions and ratings, the electrical characteristics of each gripper can be described in form of voltage balancing equation as [9]

$$V_k = R_k \cdot i_k + \frac{d\lambda_k(\theta_k, i_k)}{dt} \quad (k = 1, 2) \tag{1}$$

where $V_k$, $i_k$, $R_k$, $\lambda_k$, and $\theta_k$ are the terminal voltage, current, winding resistance, flux-linkage, and angular position of the rotor, respectively. Since the gripper works under low-speed operations, (1) can be further simplified to

$$V_k = R_k \cdot i_k + L_k(\theta_k, i_k) \cdot \frac{di_k}{dt} \quad (k = 1, 2). \tag{2}$$

From the mechanical side, each gripper can be expressed in the torque contribution form as

$$T_k = J_k \cdot \theta_k'' + K_v\theta_k' + K_s\theta_k + T_L \quad (k = 1, 2) \tag{3}$$

where $T_k$, $J_k$, $K_v$, $K_s$, and $T_L$ are the required torque, rotor inertia, damping constant, spring constant, and load torque, respectively. It can be concluded from the above representations that the SR gripper exhibits a highly nonlinear relationship from the torque output to the current and displacement.

## III. Control Strategy

### A. Online Parameter Identification

For position control applications, the gripper motion control system can be characterized as a typical second-order equation as depicted in (3), with the torque command as the input and the angular displacement as the output for each finger. Since the real-time operation is filled with noise and interference $V_k(t)$, the second-order system can be further denoted in the discrete-time form as the following [10]:

$$A(z^{-1})\theta_k = B(z^{-1})T_k + V_k(t) \quad (k = 1, 2) \tag{4}$$

where

$$\begin{cases} A(z^{-1}) = 1 + a_1 z^{-1} + a_2 z^{-2} \\ B(z^{-1}) = b_0 z^{-1} + b_1 z^{-2}. \end{cases}$$

$A(z^{-1})$ and $B(z^{-1})$ depict the denominator and nominator polynomials with parameter $a_1$, $a_2$, $b_0$, and $b_1$ to be determined. The ultimate goal of the parameter identification process is to correctly estimate the above parameters that contain system dynamics.

Based on the recursive least square (RLS) method, for any finger one, system dynamics characterized by (4) can be represented in the RLS form as

$$\theta_k^N = \Phi_k^N \cdot X_k + e_k^N \quad (k = 1, 2) \tag{5}$$

where $X = [a_1, a_2, b_0, b_1]^T$ and $\Phi_k^N = [-\theta_k^{N-1}, -\theta_k^{N-2}, T_k^{N-1}, T_k^{N-2}]$. $e_k^N$ is regarded as the $N$th stochastic residuals. For the $(N+1)$th estimation, parameters are calculated with the forgetting factor $\rho$ by the RLS method as [10]

$$\hat{X}_k^{N+1} = \hat{X}_k^N + G_k^{N+1}\left[\theta_k^{N+1} - \left(\Phi_k^{N+1}\right)^T \cdot \hat{X}_k^N\right] \tag{6}$$

$$G_k^{N+1} = \frac{P_k^N \Phi_k^{N+1}}{\rho + \left(\Phi_k^{N+1}\right)^T \cdot P_k^N \cdot \Phi_k^{N+1}} \tag{7}$$

$$P_k^{N+1} = \left[I - G_k^{N+1}\left(\Phi_k^{N+1}\right)^T\right] \cdot P_k^N / \rho \tag{8}$$

where $G$ is the gain matrix and $P$ is the covariance matrix. For the initial value of $P$, $P = \alpha \cdot I$ with $\alpha = 50$ and $I$ the $4 \times 4$ unit matrix. Termination criterion for the identification process can be set as the following with a very small positive value $\varepsilon$ as:

$$\left|\frac{\hat{X}_k^{N+1} - \hat{X}_k^N}{\hat{X}_k^N}\right| < \varepsilon. \tag{9}$$

If the maximum proportion of error from the last to the present estimated value is small when compared with the small positive number $\varepsilon$, the present value is considered to be the correct one that represents the plant model, and the estimation process will stop.

### B. Control and Drive Strategy

The pole placement technique specifies proper pole positions for the expected control performance, and the control parameters are regulated according to the designated poles [11]. The controller output and system output are determined by the reference signal through the feed-forward transfer function $T/R$ and through the feedback transfer function $S/R$, respectively. As shown in Fig. 2(a), system output $\theta_k$ and controller output $u_k$ can thus be denoted as

$$\begin{cases} \theta_k = \dfrac{BT}{AR + BS} \cdot u_k + \dfrac{BR}{AR + BS} \cdot e_k \\ u_k = \dfrac{AT}{AR + BS} \cdot u_k - \dfrac{BS}{AR + BS} \cdot e_k. \end{cases} \tag{10}$$

The closed-loop characteristic equation is $AR + BS = A_0A_m$ with causal conditions to be met as $\deg S \leq \deg R$ and $\deg T \leq \deg R$. $A_0$ stands for the observer polynomial, and $A_m$ is the desired closed-loop pole polynomial, as $A_m(z^{-1}) = 1 + a_{m1}z^{-1} + a_{m2}z^{-2}$ [11]. $R(z^{-1})$, $S(z^{-1})$, and $T(z^{-1})$ are the polynomials to be determined.

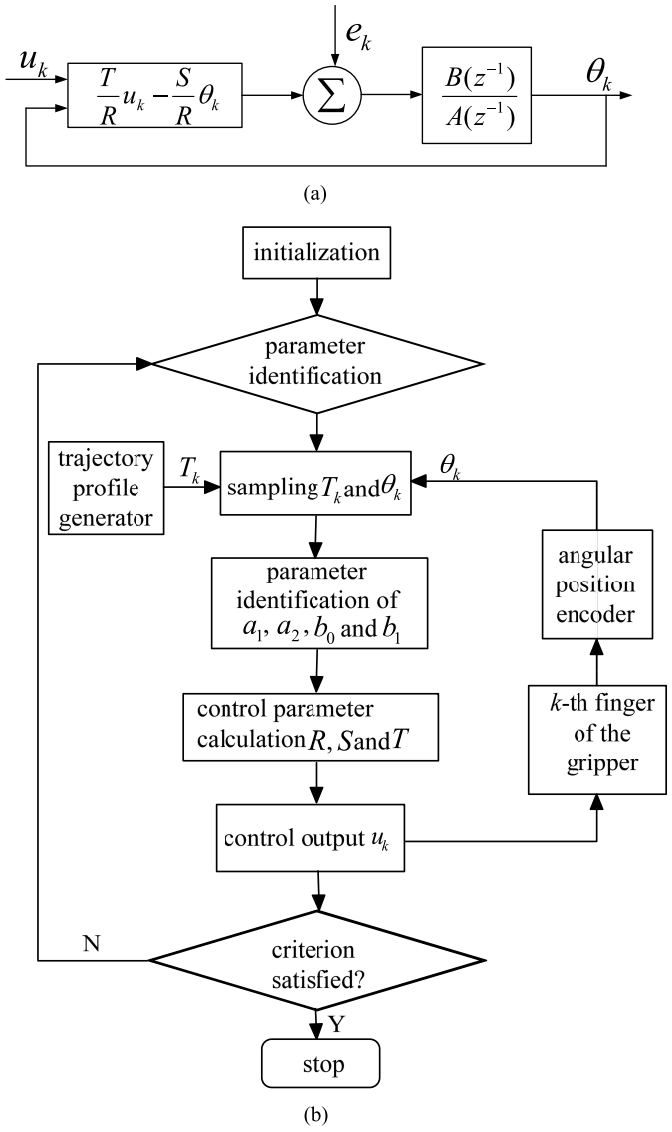


Fig. 2. (a) Control block and (b) control flow chart.

According to the constraints of the causal conditions, they can be expressed as [11]

$$\begin{cases} R = r_0 + r_1 z^{-1} \\ S = s_0 + s_1 z^{-1} \\ T = 1 + t_1 z^{-1} + t_2 z^{-2}. \end{cases} \tag{11}$$

The purpose of pole placement design is to designate the locus for the expected poles and calculate system polynomials $R$, $S$, and $T$ so that the gripper motion system follows the performance specified by the desired poles $a_{m1}$ and $a_{m2}$. The estimation and control process flow chart can thus be depicted as shown in Fig. 2(b) for each finger.

The control algorithm first samples the current torque and angular position. Then the parameter identification process starts to estimate $a_1$, $a_2$, $b_0$, and $b_1$ according to (6)–(8). Then, the polynomial coefficients of $R$, $S$, and $T$ can be determined from the algorithm of the pole placement technique [11]. Next, control output for the $k$th gripper is calculated according to (10). Meanwhile, the angular position of the $k$th gripper is fed back to the algorithm for the next calculation. If the termination criterion is met from (9), then the whole process stops and it can be regarded that the current parameters are correct.

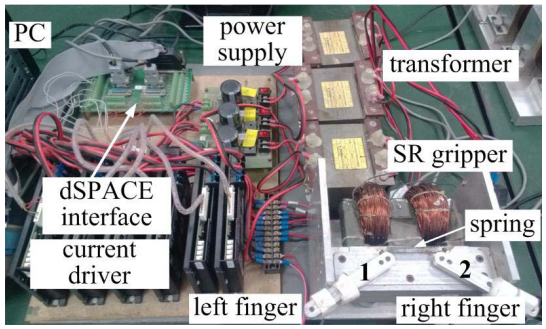


Fig. 3. Experimental setup.

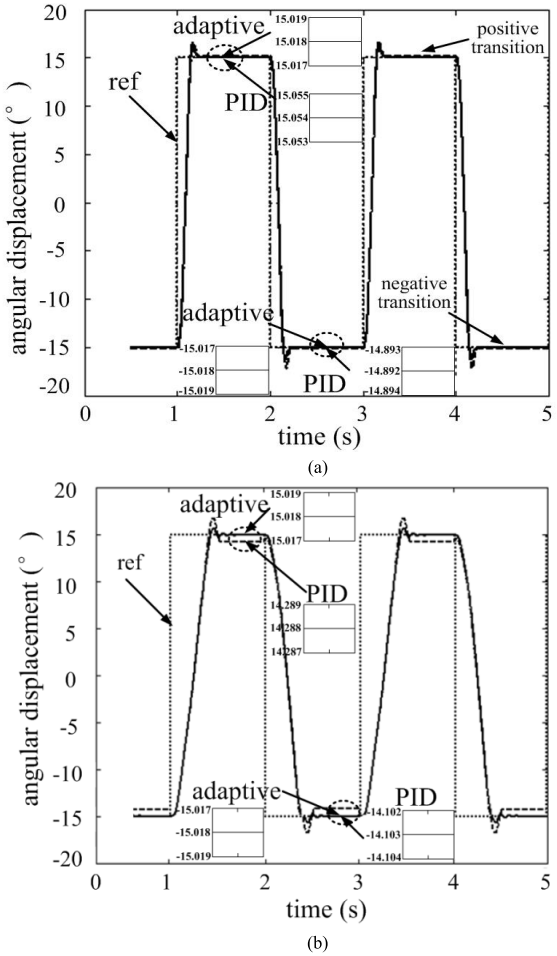


Fig. 4. Position response from (a) one finger and (b) two fingers.

## IV. Control Performance

The experiment is carried out based on a dSPACE DS1104 controller card. The whole experiment is conducted in real time and the dual-loop control strategy is applied. The outer loop is position control, and the sampling frequency is 1 kHz. The current drivers for each finger are the commercial amplifiers capable of inner current regulation based on the proportional integral algorithm, and the inner current control loop is fast enough to meet the requirements for the position control loop with a sampling rate of 10 KHz. The experimental setup can be found in Fig. 3.

TABLE II
CONTROL PERFORMANCE FOR ONE FINGER EXCITED ONLY

| Only one finger excited | PID | adaptive |
|---|---|---|
| Overshoot | 9.8% | 9.8% |
| Rising time | 0.18 s | 0.175 s |
| Tuning time (2%) | 0.26 s | 0.26 s |
| Absolute steady-state error (+ transitions) | 0.054° | 0.018° |
| Steady-state error (- transitions) | 0.108° | 0.018° |

TABLE III
CONTROL PERFORMANCE FOR TWO FINGERS SIMULTANEOUSLY EXCITED

| Two fingers simultaneously excited | PID | adaptive |
|---|---|---|
| Overshoot | 10.6% | 4.2% |
| Rising time | 0.412 s | 0.415 s |
| Tuning time (2%) | 0.63 s | 0.68 s |
| Absolute steady-state error (+ transitions) | 0.712° | 0.018° |
| Absolute steady-state error (- transitions) | 0.897° | 0.018° |

The position reference signal is a square waveform with the frequency of 0.5 Hz and the amplitude of 30° for both fingers. Since each finger has the same dimensions and ratings, the parameters for PID and the adaptive control algorithm are regulated with the same overshoot values for the left finger. The proportional, integral, and differential gains are 0.25, 0.001, and 0.032, respectively, based on a trial-and-error attempt. The coefficients $a_{m1}$ and $a_{m2}$ are thus selected as $-1.98$ and 0.98, respectively, according to the proper step response from a typical second-order system [11]. Then, the same parameters are used for the regulation of the right finger.

When the left finger is activated only, the position response waveforms can be found in Fig. 4(a). It can be seen that the profiles under the PID and the adaptive controller almost overlap during the positive transitions and the steady-state error is smaller from the adaptive control. However, during negative transitions, the overshoot is more dominant under the PID controller, since the spring begins to take effect and pulls the finger out gradually. It acts as an additional external load to the activated left finger. It is clear that both dynamic and static behaviors under the PID controller is not uniform during positive and negative transitions, and the steady-state error value increases as the spring is activated. However, the response profiles from the adaptive controller are uniform for either dynamic or static behaviors, under the entire period of operation. From the control parameters tabulated in Table II, the performance from the two controllers is similar if only one finger is excited.

Then the right finger is activated, and two fingers operate simultaneously, and the position control response waveforms for both fingers are shown in Fig. 4(b). Since the magnetic paths from the two fingers are highly coupled, each axis of motion acts as an external disturbance to another one. Therefore, the response time from the response profiles becomes slow with increased rising time. For the PID controller, there exhibits a bigger steady-state error, and the controller is not capable of high-precision position regulation, since the previous $P$, $I$, and $D$ gains are no longer suitable for the new working conditions. However, the performance under the adaptive controller still exhibits a uniform dynamic response performance, and the same static behavior with the absolute steady-state error value falling below 0.018° for both transitions can be enjoyed. It can be concluded that the adaptive controller is capable of real-time position regulation under the desired poles, and the SR gripper-based motion control system is capable of adaptation to external disturbances. The numerical data of control performance are listed in Table III for the two fingers working at the same time.

## V. CONCLUSION AND DISCUSSION

This paper first investigates a two-finger gripper based on SR technology with a simple and robust mechanical machine structure. Since the two fingers share a common magnetic path, one finger acts as a time-variant, external load disturbance to another. The adaptive position controller based on online parameter identification is capable of real-time regulation, error correction, and adaption to external disturbances. Experimental results with performance comparison between a traditional PID controller proves that the proposed controller can achieve a uniform control performance either for one or for both fingers, with an absolute steady-state error value within 0.018°. Therefore, there is no need for the introduction of any decoupling mechanisms for the SR gripper to obtain a uniform, high-precision position control performance under the proposed adaptive controller.

## ACKNOWLEDGMENT

This work was supported in part by the National Natural Science Foundation of China, in part by the Guangdong Natural Science Foundation under Project 51477103 and Project S2014A030313564, in part by the Shenzhen Government, and in part by the PolyU Research Fund under Grant JCYJ20130329144017199 and Grant 4-ZZD6.

## REFERENCES

[1] T. Chen, L. Chen, L. Sun, and X. Li, "Design and fabrication of a four-arm-structure MEMS gripper," *IEEE Trans. Ind. Electron.*, vol. 56, no. 4, pp. 996–1004, Apr. 2009.
[2] J. R. Amend, E. M. Brown, N. Rodenberg, H. M. Jaeger, and H. Lipson, "A positive pressure universal gripper based on the jamming of granular material," *IEEE Trans. Robot.*, vol. 28, no. 2, pp. 341–350, Apr. 2012.
[3] N. Geismar, M. Dawande, and C. Sriskandarajah, "Productivity improvement from using machine buffers in dual-gripper cluster tools," *IEEE Trans. Autom. Sci. Eng.*, vol. 8, no. 1, pp. 29–41, Jan. 2011.
[4] J. Becedas, I. Payo, and V. Feliu, "Two-flexible-fingers gripper force feedback control system for its application as end effector on a 6-DOF manipulator," *IEEE Trans. Robot.*, vol. 27, no. 3, pp. 599–615, Jun. 2011.
[5] H. Terasaki and T. Hasegawa, "Motion planning of intelligent manipulation by a parallel two-fingered gripper equipped with a simple rotating mechanism," *IEEE Trans. Robot. Autom.*, vol. 14, no. 2, pp. 207–219, Apr. 1998.
[6] A. E. Fitzgerald and C. Kingsley, Jr., *Electric Machinery*. Tokyo, Japan: McGraw-Hill, 1961, pp. 78–85.
[7] M. Stewart, M. G. Cain, and W. Battrick, "Surface displacement mapping of piezoelectric multilayer actuators," in *Proc. IEEE 8th Int. Conf. Dielectr. Mater., Meas. Appl.*, Sep. 2000, pp. 445–447.
[8] K. K. Chan and N. C. Cheung, "A novel two-finger variable-reluctance gripper for high-speed grasping of delicate objects: An implementation case study," *IEEE Trans. Ind. Electron.*, vol. 52, no. 6, pp. 1705–1707, Dec. 2005.
[9] R. Krishan, *Switched Reluctance Motor Drives: Modeling, Simulation, Analysis, Design, and Applications*. New York, NY, USA: CRC Press, 2001, pp. 5–8.
[10] L. Ljung, *System Identification: Theory for the User*, 2nd ed. New York, NY, USA: Prentice-Hall, 1998, pp. 193–195.
[11] K. J. Åström and B. Wittenmark, *Adaptive Control*, 2nd ed. London, U.K.: Addison-Wesley, 1995, pp. 78–85.